

# Environment Dependent Interatomic Potential for Bulk Silicon

Martin Z. Bazant<sup>†</sup>, Efthimios Kaxiras<sup>†</sup> and J. F. Justo<sup>‡</sup>

<sup>†</sup> *Department of Physics, Harvard University, Cambridge, MA 02138*

<sup>‡</sup> *Department of Nuclear Engineering, Massachusetts Institute of Technology, Cambridge, MA 02139*  
(April 16, 1997)

We use recent theoretical advances to develop a new functional form for interatomic forces in bulk silicon. The theoretical results underlying the model include a novel analysis of elastic properties for the diamond and graphitic structures and inversions of *ab initio* cohesive energy curves. The interaction model includes two-body and three-body terms which depend on the local atomic environment through an effective coordination number. This formulation is able to capture successfully: (i) the energetics and elastic properties of the ground state diamond lattice; (ii) the covalent re-hybridization of undercoordinated atoms; (iii) and a smooth transition to metallic bonding for overcoordinated atoms. Because the essential features of chemical bonding in the bulk are built into the functional form, this model promises to be useful for describing interatomic forces in silicon bulk phases and defects. Although this functional form is remarkably realistic by usual standards, it contains a small number of fitting parameters and requires computational effort comparable to the most efficient existing models. In a companion paper, a complete parameterization of the model is given, and excellent performance for condensed phases and bulk defects is demonstrated.

## I. INTRODUCTION

The study of materials properties is increasingly relying on a microscopic description of the underlying atomic structure and dynamics. While many of the key features can be described by a small number of atoms that are actively participating in a physical process, many problems of interest require of order  $10^3$ – $10^6$  or even higher number of atoms and time scales of 10-100 *ps* for a proper description. *Ab initio* methods based on density functional theory<sup>1</sup> and the local density approximation (DFT/LDA) have been intensively and successfully used to provide a microscopic description of simple structures<sup>2</sup>. For more complex cases, including for instance disordered or stepped surfaces, dislocations, grain boundaries, crystal growth and the amorphous-to-crystal transition, a large number of atoms is required, making an *ab initio* description untenable. A possible alternative for these cases might be empirical interatomic potentials which are computationally much less expensive. The difficulty in employing empirical potentials is their unproven ability to capture the physics of structures far from the fitting data used to construct them. Developing reliable empirical potentials remains an issue of great interest and possibly of great rewards.

Silicon is a test case for the development of empirical potentials for covalent materials. Its great technological importance, the vast amount of relevant experimental and theoretical studies available, and its intrinsic interest as the representative covalent material make it an ideal candidate for exploring to what extent the empirical potential approach can be exploited. In recent years, more than 30 empirical potentials for silicon have been developed and applied to a number of different systems, and

more recently compared to each other<sup>3,4</sup>. They differ in degree of sophistication, functional form, fitting strategy and range of interaction, and each can accurately model various special atomic configurations. Surfaces and small clusters are the most difficult to handle<sup>3,5</sup>, but even bulk material (crystalline and amorphous phases, solid defects and the liquid phase) has resisted a transferable description by a single potential. Realistic simulations of important bulk phenomena such as plastic deformation, diffusion and crystallization are still problematic.

In this article, we derive a general model for the functional form of interatomic forces in bulk tetrahedral semiconductors. This functional form is applied to the prototypical case of silicon in a companion article<sup>6</sup>. The development of the model is organized as follows: In section II, we briefly review existing potentials and approximations of quantum models for silicon and extract important conclusions about the desirable features of a successful interatomic potential. Recent theoretical advances used in deriving our model from *ab initio* total energy data are outlined in section III. A functional form that incorporates the theoretical results using a minimal number of fitting parameters is presented and discussed in section IV. Finally, section V contains some concluding remarks.

## II. REVIEW OF EMPIRICAL POTENTIALS AND APPROXIMATIONS

### A. Empirical Potentials

The usual approach for deriving empirical potentials is to guess a functional form, motivated by physical intuition, and then to adjust parameters to fit *ab initio* total

energy data for various atomic structures. A covalent material presents a difficult challenge because complex quantum-mechanical effects such as chemical bond formation and rupture, hybridization, metalization, charge transfer and bond bending must be described by an effective interaction between atoms in which the electronic degrees of freedom have somehow been “integrated out”<sup>7</sup>. In the case of Si, the abundance of potentials in the literature illustrates the difficulty of the problem and lack of specific theoretical guidance. In spite of the wide range of functional forms and fitting strategies, all proposed models possess comparable (and insufficient) overall accuracy<sup>3</sup>. It has proven almost impossible to attribute the successes or failures of a potential to specific features of its functional form. Nevertheless, much can be learned from past experience, and it is clear that a well-chosen functional form is more useful than elaborate fitting strategies.

To appreciate this point we compare and contrast some representative potentials for silicon. The pioneering potential of Stillinger and Weber (SW) has only eight parameters and was fitted to a few experimental properties of solid cubic diamond and liquid silicon<sup>8</sup>. The model takes the form of a third order cluster potential<sup>7</sup> in which the total energy of an atomic configuration  $\{\vec{R}_{ij}\}$  is expressed as a linear combination of two- and three-body terms,

$$E = \sum_{ij} V_2(R_{ij}) + \sum_{ijk} V_3(\vec{R}_{ij}, \vec{R}_{ik}), \quad (1)$$

where  $\vec{R}_{ij} = \vec{R}_j - \vec{R}_i$ ,  $R_{ij} = |\vec{R}_{ij}|$  and we use the convention that multiple summation is over all permutations of distinct indices. The range of the SW potential is just short of the second neighbor distance in the equilibrium DC lattice, so the pair interaction  $V_2(r)$  has a deep well at the first neighbor distance to represent the restoring force against stretching  $sp^3$  hybrid covalent bonds. The three-body interaction is expressed as a separable product of radial functions  $g(r)$  and an angular function  $h(\theta)$

$$V_3(\vec{r}_1, \vec{r}_2) = g(r_1)g(r_2)h(l_{12}), \quad (2)$$

where  $l_{12} = \cos\theta_{12} = \vec{r}_1 \cdot \vec{r}_2 / (r_1 r_2)$ . The angular function,  $h(l) = (l + 1/3)^2$ , has a minimum of zero at the tetrahedral angle to represent the angular preference of  $sp^3$  bonds, and the radial function  $g(r)$  decreases with distance to reduce this effect when bonds are stretched. The SW three-body term captures the directed nature of covalent  $sp^3$  bonds in a simple way that selects the diamond lattice over close-packed structures. Although the various terms lose their physical significance for distortions of the diamond lattice large enough to destroy  $sp^3$  hybridization, the SW potential seems to give a reasonable description of many states experimentally relevant, such as point defects, certain surface structures, and the liquid and amorphous states<sup>3</sup>. The SW potential continues to be a favorite choice in the literature, due in large

part to its appealing simplicity and apparent physical content.

Another popular and innovative empirical model is the Tersoff potential, with three versions generally called T1<sup>9</sup>, T2<sup>10</sup>, and T3<sup>11</sup>. The original version T1 has only six adjustable parameters, fitted to a small database of bulk polytypes. Subsequent versions involve seven more parameters to improve elastic properties. The Tersoff functional form is fundamentally different from the SW form in that the strength of individual bonds is affected by the presence of surrounding atoms. Using Carlson’s terminology, the Tersoff potential is a third order cluster functional<sup>7</sup> with the cluster sums appearing in nonlinear combinations. As suggested by theoretical arguments<sup>12–14</sup>, the energy is the sum of a repulsive pair interaction  $\phi_R(r)$  and an attractive interaction  $p(\zeta)\phi_A(r)$  that depends on the local bonding environment, which is characterized by a scalar quantity  $\zeta$ ,

$$E = \sum_{ij} [\phi_R(R_{ij}) + p(\zeta_{ij})\phi_A(R_{ij})] \quad (3)$$

$$\zeta_{ij} = \sum_k V_3(\vec{R}_{ij}, \vec{R}_{ik}), \quad (4)$$

where the function  $p(\zeta)$  represents the Pauling bond order. The three-body interaction has the form of Eq. (2) with the important difference that the angular function, although still positive, may not have a minimum at the tetrahedral angle. The T1, T2 and T3 angular functions are qualitatively different, possessing minima at 180°, 90° and 126.745°, respectively. The Tersoff format has greater theoretical justification away from the diamond lattice than SW, but the three versions do not outperform the SW potential overall, perhaps due to their handling of angular forces<sup>3</sup>. Nevertheless, the Tersoff potential is another example of a successful potential for bulk properties with a physically motivated functional form and simple fitting strategy.

The majority of empirical potentials fall into either the generic SW<sup>15–17</sup> or Tersoff<sup>18–22</sup> formats just described, but there are notable exceptions that provide further insight into successful approaches for designing potentials. First, a number of potentials possess functional forms that have either limited validity or no physical motivation at all, suggesting that fitting without theoretical guidance is not the optimal approach. The Valence Force Field<sup>23,24</sup> and related potentials<sup>25,26</sup> (of which there are over 40 in the literature<sup>25</sup>) involve scalar products of the vectors connecting atomic positions, an approximation that is strictly valid only for small departures from equilibrium. Thus, extending these models to highly distorted bonding environments undermines their theoretical basis. The potential of Pearson *et. al.*<sup>27</sup>, as the authors emphasize, is not physically motivated, but rather results from an exercise in fitting. Their use of Lennard-Jones two-body terms and Axilrod-Teller three-body terms, characteristic of Van der Waals forces, has no justification for covalent materials. The potential of Mis-

triotis, Flytzanis and Farantos (MFF)<sup>28</sup> is an interesting attempt to include four-body interactions. Although the importance of four-body terms is certainly worth exploring, the inclusion of a four-body term in a linear cluster expansion is not unique, and theoretical analysis tends to favor nonlinear functionals<sup>7,13,14</sup>.

A natural strategy to improve on the SW and Tersoff models is to replace simple functional forms with more flexible ones and complement them with more elaborate fitting schemes. The Bolding and Andersen (BA) potential<sup>29</sup> generalizes the Tersoff format with over 30 adjustable parameters fit to an unusually wide range of structures. Although it has not been thoroughly tested, the BA potential appears to describe simultaneously bulk phases, defects, surfaces and small clusters, a claim that no other potential can make<sup>3</sup>. However, its complexity makes it difficult to interpret physically, and since a large fitting database was used, it is unclear whether the potential can reliably describe structures to which it was not explicitly fit. In this vein, the spline-fitted potentials of the Force Matching Method<sup>30</sup> represent the opposite extreme of the SW and Tersoff approaches: physical motivation is bypassed in favor of elaborate fitting. These potentials involve complex combinations of cubic splines, which have effectively hundreds of adjustable parameters, and the strategy of matching forces on all atoms in various defect structures is the most elaborate attempted thus far. Although the method may be worth pursuing as an alternative, it has not yet produced competitive potentials<sup>31</sup>. Moreover, even if a reliable potential could result from such fitting strategies, it would make it hard to interpret the results of atomistic simulations in terms of simple principles of chemical bonding. Such interpretation is essential, in our view, if physical insight is to be gained from computer simulations.

In spite of relentless efforts, no potential has demonstrated a transferable description of silicon in all its forms<sup>3</sup> leading us to another important conclusion: it may be too ambitious to attempt a simultaneous fit of all of the important atomic structures (bulk crystalline, amorphous and liquid phases, surfaces, and clusters) since qualitatively different aspects of bonding are at work in different types of structures. Theory and general experience suggest that the main ingredient needed to differentiate between surface and bulk bonding preferences is a more sophisticated description of the local atomic environment. A notable example in this respect is the innovative Thermodynamic Interatomic Force Field (TIFF) potential of Chelikowsky *et. al.*<sup>32</sup>, which includes a quantity called the “dangling bond vector” that is a weighted average of the vectors pointing to the neighbors of an atom. For symmetric configurations characteristic of the ideal (or slightly distorted) bulk material, the dangling bond vector vanishes (or is exceedingly small). Conversely, a nonzero value of the dangling bond vector indicates an asymmetric distribution of neighbors. While the TIFFF dangling bond vector description appears to be very useful for undercoordinated structures like surfaces

and small clusters, in this work we restrict ourselves to bulk material and thus use a simpler, scalar environment description. Our goal is to obtain the best possible description of condensed phases and defects with a simple, theoretically justified functional form.

## B. Approximation of Quantum Models

An alternative to fitting guessed functional forms is to derive potentials by systematic approximation of quantum-mechanical models. So far, this approach has failed to produce superior potentials, but important connections between electronic structure and effective interatomic potentials have been revealed. Although attempts are being made to directly approximate Density Functional Theory<sup>33</sup>, the most useful contributions involve approximating various Tight Binding (TB) models, which can themselves be derived as approximations of first principles theories<sup>34</sup>. These methods are based on low order moment approximations of the TB local density of states (LDOS), which is used to express the average band energy as the sum of occupied bonding states<sup>7,14,35–39</sup>. Pettifor has derived a many-body potential, similar in form to the Tersoff potential, by approximation of the TB bond order<sup>14</sup>. More recently, an angular dependence remarkably close to the T3 angular function has been derived for  $\sigma$  bonding from the lowest order two-site term in the Bond Order Potential expansion<sup>35</sup>, but the analytically derived function has a flat minimum around  $130^\circ$  and thus differs qualitatively with the T1 and T2 potentials. With hindsight, a simple physical principle explains these results: a  $\sigma$  bond is most weakened (desaturated) by the presence of another atom when the resulting angle is small ( $\theta < 100^\circ$ ) because in such cases the atom lies near the bond axis, thus interfering with the  $\sigma$  orbital where it is most concentrated. Working within the same framework of the TB LDOS, Carlsson and coworkers have derived potentials with the Generalized Embedded Atom Method<sup>36–38</sup>. Harrison has arrived at a similar model by expanding the average band energy in the ratio of the width of the bonding band to the bond-antibond splitting, the relevant small parameter in semiconductors<sup>39</sup>. These potentials resemble the SW potential in its description of angular forces with an additive three-body term, particularly for small distortions of the diamond lattice. The transition to metallic behavior in overcoordinated structures involves interbond interactions similar to the Tersoff and embedded atom potentials.

Many-body potentials can be derived from quantum-mechanical models if we restrict our attention to important small sets of configurations. Using a basis of  $sp^3$  hybrid orbitals in a TB model, Carlsson *et. al.*<sup>7,36</sup> have shown that a generalization of the SW format, in which Eq. (2) is replaced by a form similar to that used by Biswas and Hamann (BH)<sup>15</sup>,

$$V_3(\vec{r}_1, \vec{r}_2) = \sum_{m=0}^2 g_m(r_1)g_m(r_2) l_{12}^m, \quad (5)$$

is valid in the vicinity of the equilibrium diamond lattice. In general, the fourth moment controls the essential band gap of a semiconductor, implying four-body interactions, but the separable, three-body SW/BH terms are a consequence of the open topology of the diamond lattice: the only four-atom hopping circuit between first neighbors is the self-retracing path  $i \rightarrow j \rightarrow i \rightarrow k \rightarrow i$ .

We can make analogous arguments for the graphitic lattice to draw conclusions about  $sp^2$  hybrid bonds. Ignoring the weak, long-range interaction between hexagonal planes, we can assume a TB basis of  $sp^2$  hybrid orbitals and follow Carlsson’s derivation. Because the self-retracing path is also the only first neighbor hopping circuit in a graphitic plane, a cluster expansion with the generic BH three-body interaction is also valid for hexagonal configurations, with the functions in Eqs. (1) and (5) differing from their diamond  $sp^3$  counterparts, as described below. These calculations also suggest that a locally valid cluster expansion should acquire strong environment dependence for large distortions from the reference configuration<sup>7</sup>.

These studies provide theoretical evidence that the linear three-body SW/BH format is appropriate near equilibrium structures, while the nonlinear many-body Tersoff format describes general trends across different bulk structures. For the asymmetric configurations found in surfaces and small clusters, these theories also suggest that a more complicated environment dependence than Tersoff’s is needed, like the dangling bond vector of the TIFF potential<sup>14,36</sup>. In conclusion, direct approximation of quantum models can provide insight into the origins of interatomic forces, but apparently cannot produce improved potentials. The reason may be that the long chain of approximations connecting first principles and empirical theories is uncontrolled, in the sense that there is no small parameter which can provide an asymptotic bound for the neglected terms for a wide range of configurations<sup>40</sup>.

### III. INVERSION OF *AB INITIO* ENERGY DATA

There are very few hard facts concerning the nature of interatomic forces. Although there has been a proliferation of *ab initio* energy and force calculations for a wide range of atomic structures, it has proven difficult to discover any concrete information regarding the functional form of interatomic potentials. With the ubiquitous fitting approach, it is never clear whether discrepancies with *ab initio* data result from an incorrect functional form or simply suboptimal fitting<sup>3</sup>. Thus, in addition to the practical problem of designing potentials, it is also difficult to build a simple conceptual framework within which to understand the complexities of chemical bonding. In this section, we summarize our recent

efforts to extract features of interatomic forces directly from *ab initio* total energy data. In order to investigate the global trends in bonding across bulk structures predicted by quantum theories, we first perform inversions of *ab initio* cohesive energy curves in part III A. By analyzing elastic properties of covalent solids in part III B, we then explore the cohesive forces in certain special (high symmetry) bonding states, which can be viewed as an inversion of *ab initio* energies restricted to selected important configurations.

#### A. Inversion of Cohesive Energy Curves

We have recently shown that it is possible to derive effective interatomic potentials for covalent solids directly from *ab initio* data<sup>41,42</sup>. The inversion procedure generalizes the “*ab initio* pair potential” of Carlsson, Gelatt and Ehrenreich<sup>43</sup> to many-body interactions and for arbitrary strains beyond uniform volume expansion<sup>44</sup>. For the case of silicon, this work provides first principles evidence in favor of the generic bond order form of the pair interaction,

$$V_2(r, Z) = \phi_R(r) + p(Z)\phi_A(r), \quad (6)$$

where  $\phi_R(r)$  represents the short-range repulsion of atoms due to Pauli exclusion of their electrons,  $\phi_A(r)$  represents the attractive force of bond formation, and  $p(Z)$  is the bond order, which determines the strength of the attraction as a function of the atomic environment, measured by the coordination  $Z$ . The theoretical behavior of the bond order is as follows<sup>7,13,14,37,38</sup>: The ideal coordination for Si is  $Z_0 = 4$ , due to its valence. As an atom becomes increasingly overcoordinated ( $Z > Z_0$ ), nearby bonds become more metallic, characterized by delocalized electrons. In terms of electronic structure, the LDOS for overcoordinated atoms can be reasonably well described by its scalar second moment. It is a well established result that the leading order behavior of the bond order is  $p(Z) \sim Z^{-1/2}$  in the second moment approximation<sup>7,14,38</sup>. For  $Z \leq Z_0$  on the other hand, a matrix second moment treatment predicts a roughly constant bond order (additive bond strengths)<sup>36</sup>. For small coordinations higher moments are needed to incorporate important features of band shape characteristic of covalent bonding, primarily the formation of a gap in the LDOS<sup>7,14,36,37</sup>. Thus, the bond order should depart from the divergent  $Z^{-1/2}$  behavior at lower coordinations with a shoulder at the ideal coordination of  $Z = Z_0$  where the transition to metallic  $Z^{-1/2}$  dependence begins.

Inversion of *ab initio* cohesive energy curves verifies that trends in chemical bonding across various bulk bonding arrangements are indeed consistent with these theoretical predictions<sup>41</sup>. Previously, the only evidence in support of the bond order formalism came from *equilibrium* bond lengths and energies for a small set of ideal

crystal structures<sup>9–11,13,19</sup>. The inversion approach has revealed for the first time that the bond order decomposition expressed by Eq. (6) is actually valid for a wide range of volumes away from equilibrium and for a representative set of low energy crystal structures. In addition to selecting the generic form of the pair interaction, inversion provides a precise measure of the relative bond orders in various local atomic configurations. For example, the bond order of  $sp^2$  bonds involving three-fold coordinated atoms is about 5% greater than that of four-fold coordinated  $sp^3$  bonds in silicon.

These results have immediate implications for empirical potentials. The main conclusion is that the generic Tersoff format is much more realistic than the SW format for highly distorted configurations. However, the inversion results also indicate that a coordination-dependent pair interaction can provide a fair description of high-symmetry crystal structures without requiring additional many-body interactions. In particular, angular forces are only needed to stabilize these structures under symmetry-breaking distortions, primarily for small coordinations. In order to make a quantitative connection between Tersoff’s functional form and our inverted *ab initio* data, angular contributions to the bond order must somehow be suppressed for ideal crystal structures.

The inversion procedure applied to explicit three-body interactions has also led to some useful conclusions. Although it is not always the case<sup>42</sup>, inverted three-body radial functions  $g(r)$  tend to be strictly decreasing functions (like SW), especially when an overdetermined set of input structures is used<sup>41</sup>. Inverted angular functions  $h(l)$  also tend to penalize small angles ( $\theta < \pi/2$ ) less than most existing models, in agreement with a comparative study of empirical potentials<sup>3</sup>. We must emphasize, however, that the results of this section concern general trends in chemical bonding, and have little to offer in terms of the precise nature of interatomic forces in special atomic configurations, such as the low-energy states of hybrid covalent bonds. To understand better these critical cases, we employ a related inversion strategy.

## B. Analysis of Elastic Properties

A useful theoretical approach to guide the development of potentials, which has been pursued recently only by Cowley<sup>45</sup>, is to predict elastic properties implied by generic functional forms and compare with experimental or *ab initio* data. This tool for understanding interatomic forces dates back to the 19th century, when St. Venant showed that the assumption of central pairwise forces supported by Cauchy and Poisson implied a reduction in the number of independent elastic constants from 21 to 15<sup>46</sup>. The corresponding six dependencies, given by the single equation  $C_{12} = C_{44}$  if atoms are at centers of cubic symmetry, are commonly called the Cauchy relations<sup>46,47</sup>. They provide a simple test for selecting

which materials can be described by a pair potential<sup>48,49</sup>. Once it was realized that the Cauchy relations are not satisfied by the experimental data for semiconductors, a number of authors in this century, led by Born<sup>50,51</sup>, derived generalized Cauchy relations for noncentral forces in the diamond structure<sup>52,48</sup>. Building upon this body of work, we have recently analyzed the elastic properties of several general classes of many-body potentials in the diamond and graphitic crystal structures in order to gain insight into the mechanical behavior of  $sp^3$  and  $sp^2$  hybrid covalent bonds, respectively<sup>44</sup>. These high symmetry atomic configurations must be accurately described by any realistic model of interatomic forces in a tetravalent solid. Here we will only outline results directly related to the model presented in the next section.

*sp<sup>3</sup> Hybrids*: Consider one of the simplest many-body interaction models for a tetrahedral solid, that is the generic SW format defined in Eqs. (1) and (2), with nearest neighbor interactions and an angular function having a minimum of zero at the tetrahedral angle ( $h = h' = 0, h'' > 0$ ). In that case, first considered by Harrison<sup>48,53</sup>, the functional form of the potential has only two degrees of freedom for elastic behavior,  $V_2''$  and  $h''$ , the curvatures of the pair interaction and of the angular function at their respective minima<sup>45</sup>. Since cubic symmetry allows for three independent elastic moduli, there is an implied relation, due to Harrison,

$$(7C_{11} + 2C_{12})C_{44} = 3(C_{11} + 2C_{12})(C_{11} - C_{12}). \quad (7)$$

Using the experimental data<sup>54</sup> shown in Table I, the ratio of the two sides of the Harrison relation is 1.16, indicating a reasonable description by a simple SW model. In contrast, the potentials with the Tersoff format, T2, T3 and Dodson (DOD)<sup>18</sup>, are far from satisfying this relation. This does not imply rejection of the Tersoff format, because the functional form has more than enough degrees of freedom to exactly reproduce all the elastic constants. However, as such, the inability of Tersoff potentials to accurately describe elastic behavior when constrained to fit other important properties does suggest a potential shortcoming in the functional form.

A more compelling reason to select the SW format over others in the literature comes from the unrelaxed shear modulus  $C_{44}^0$  which does not include relaxation of the internal degrees of freedom in the crystal unit cell. In the early literature on elastic forces, unrelaxed elastic moduli were ignored, because they are not experimentally accessible. With the advent of *ab initio* calculations that predict elastic constants within a few percent of experimental values, we can now analyze unrelaxed elastic properties as well. Considering again the simple SW format, with its two degrees of freedom, we have discovered another relation for the unrelaxed moduli,

$$4C_{11} + 5C_{12} = 9C_{44}^0. \quad (8)$$

As shown in Table I, *the experimental and ab initio elastic moduli satisfy this relation* within experimental and

computational error. On the other hand, more general cluster potentials and functionals, including the Tersoff format, BH and PTHHT, do not require this relation, and in fact cannot satisfy it under the usual circumstances. This is demonstrated in Table I and explains why it has proven difficult to obtain good elastic properties with the Tersoff potential<sup>56</sup>. These results unambiguously select the SW format with first neighbor interactions for describing small homogeneous strains of the diamond lattice. Although imperfect, internal relaxation with the SW format is also much better than with other models. Combining Eqs. (7) and (8), we arrive at a relation involving all four moduli,  $C_{11}$ ,  $C_{12}$ ,  $C_{44}$  and  $C_{44}^0$ ,

$$C_{44}^0 - C_{44} = \frac{(C_{11} + 8C_{12})^2}{9(7C_{11} + 2C_{12})}, \quad (9)$$

that expresses the effect of internal relaxation. If the two degrees of freedom in the SW format are used to reproduce the experimental values of  $C_{11}$  and  $C_{12}$ , and thus also  $C_{44}^0$  by Eq. (8), then the predicted value of  $C_{44}$  from Eq. (9) is 0.71 Mbar, which is only 12% smaller than the experimental value of 0.81 Mbar. The elastic behavior of the SW format is quite remarkable considering it has only half of the necessary degrees of freedom, while most other models are overdetermined for elastic behavior. This explains the surprising fact<sup>3</sup> that the SW potential gives one of the best descriptions of elastic properties in spite of not having been fit to any elastic constants. We conclude that it is the superiority of the simple SW functional form that gives the desirable properties, not a complex fitting procedure.

Using analytic expressions for the elastic constants it is possible to devise a simple prescription to achieve good elastic properties with the SW format. As a simple consequence of  $h(-1/3) = 0$ , the curvature of the pair potential is given by,

$$\phi''(r_d) = \frac{3V_d}{4r_d^2}(C_{11} + 2C_{12}). \quad (10)$$

The curvature of the angular function can be related to the second shear modulus<sup>57</sup>,

$$g(r_d)^2 h''(-1/3) = \frac{9V_d}{32}(C_{11} - C_{12}), \quad (11)$$

where  $r_d$ ,  $a_d$  and  $V_d = a_d^3/8$  denote the equilibrium first neighbor distance, lattice constant and atomic volume. Using the *ab initio* data in Table I, the right hand sides of Eqs. (10) and (11) evaluate to 8.1 eV/Å<sup>2</sup> and 5.7 eV, respectively. This provides a simple two-step procedure to maintain good elastic behavior while fitting any model with the SW format near the diamond lattice: (i) scale the pair interaction  $V_2(r)$  to obtain the correct bulk modulus  $K = (C_{11} + 2C_{12})/3$ , and (ii) scale the three-body energy to set the second shear modulus. As shown above, this will lead to perfect unrelaxed elastic constants and only a 12% error in  $C_{44}$ .

*sp<sup>2</sup> Hybrids:* We have also obtained useful information about interatomic forces due to *sp<sup>2</sup>* hybrid bonds from the elastic moduli of the graphitic structure<sup>44</sup>. In this analysis we neglect interplanar interactions, which are insignificant compared to the covalent bonds within a single, hexagonal plane. Our goal is to understand the elastic properties of *sp<sup>2</sup>* hybrids appearing around three-fold coordinated atoms in a bulk environment, such as a dislocation core or a grain boundary<sup>58</sup>. An isolated hexagonal plane embedded in three-dimensional space has three independent (unrelaxed) elastic constants,  $C_{11}$ ,  $C_{12}$ , and  $C_{44}^0$  with units of energy per unit area<sup>59</sup>. It can be shown that  $C_{44}^0 = 0$  for any three-body cluster potential or functional, in perfect agreement with the vanishing *ab initio* value<sup>60</sup>. There is no relation for the remaining constants,  $C_{11}$  and  $C_{12}$ , implied by empirical models because each functional form possesses at least two degrees of freedom.

Drawing on the TB approximations described above, which correctly predict the general form of interactions mediated by *sp<sup>3</sup>* hybrids, we proceed by assuming a separate three-body cluster potential for *sp<sup>2</sup>* hybrids given by Eqs. (1) and (5). By analogy with the *sp<sup>3</sup>* case, we further assume the simpler SW form of Eq. (2) for the three-body interaction, with the important difference that the angular function has a minimum of zero at the *hexagonal angle* of  $2\pi/3$  rather than at the tetrahedral angle. We again restrict the interaction range to nearest neighbors engaged in the covalent bonds that dominate cohesion. These are not the only possible choices, but we can evaluate their validity through analysis of elastic moduli.

With such a functional form<sup>61</sup>, which differs from all existing empirical potentials<sup>62</sup>, stability considerations imply  $C_{11} > 3C_{12}$ , which is indeed satisfied by the *ab initio* values,  $C_{11} = 1.79$  Mbar and  $C_{12} = 0.51$  Mbar<sup>60</sup>. More importantly, we can relate the mechanical properties of *sp<sup>2</sup>* and *sp<sup>3</sup>* hybrids. The relative radial stiffness is given by a simple ratio of elastic constants,

$$\frac{\phi_h''(r_h)}{\phi_d''(r_d)} = \frac{8r_d^2}{9r_h^2} \frac{A_h(C_{11} + C_{12})_h}{V_d(C_{11} + 2C_{12})_d}, \quad (12)$$

where the subscript  $h$  refers to the equilibrium hexagonal plane with area per atom  $A_h = a_h^2\sqrt{3}/4$ , and  $d$  refers to the diamond lattice. Using the *ab initio* result,  $r_h = 2.23$ Å, the prefactor in Eq. (12) is 0.99, so the elastic constant ratio in parentheses provides a direct comparison of *sp<sup>2</sup>* and *sp<sup>3</sup>* radial forces. The *ab initio* value of that ratio is  $1.4 \pm 0.1$ , implying that *sp<sup>2</sup>* bonds have 40% greater radial stiffness than *sp<sup>3</sup>* bonds. The same result also follows directly from inverted pair potentials for the graphitic and diamond structures<sup>41</sup>.

A similar elastic analysis yields an expression for the relative angular stiffness of *sp<sup>2</sup>* and *sp<sup>3</sup>* hybrid bonds,

$$\frac{h_h''(-1/2)}{h_d''(-1/3)} = \frac{256g_d(r_d)^2}{243g_h(r_h)^2} \frac{A_h(C_{11} - 3C_{12})_h}{V_d(C_{11} - C_{12})_d}, \quad (13)$$

Using the *ab initio* data, we have the general result,  $g_h(r_h)^2 h_h''(-1/2)/g_d(r_d)^2 h_d''(-1/3) = 0.46 \pm 0.15$ . Assuming  $g_d(r) \approx g_h(r)$  with each function decreasing in accordance with inversion results<sup>41</sup>, then the product of prefactors in Eq. (13) is nearly unity. In that case the ratio of elastic constants in parentheses allows us to quantify the relative bending strength of the hybrid bonds. The *ab initio* value for the ratio of  $0.44 \pm 0.15$  indicates that the angular stiffness of  $sp^2$  bonds is smaller than that of  $sp^3$  bonds by about a factor of two, in spite of the greater radial stiffness of  $sp^2$  bonds. Our conclusion for the relative bending strength of  $sp^2$  and  $sp^3$  hybrids would be reversed only if  $g_g(r_g)$  were smaller than  $g_d(r_d)$  by at least a factor of two, which seems unlikely in light of the bond orders.

Elastic constant analysis suggests that a hybrid covalent bond is well represented by a separable, first-neighbor, three-body cluster potential whose angular function has a minimum of zero at the appropriate angle. This may seem to contradict the ample evidence we have cited in favor of the Tersoff format for large distortions of the diamond lattice, particularly those involving changes in coordination. These findings are consistent, however, in light of Carlsson’s argument that cluster potentials like SW can accurately fit narrow ranges of configurations while cluster functionals like Tersoff’s provide a less accurate but physically acceptable fit to a much broader set of configurations<sup>63</sup>.

This body of results forms a reliable foundation upon which to build empirical potentials for bulk tetravalent solids. In general, we conclude that the functional form of atomic interactions should reduce exactly to appropriate cluster potentials in special bonding geometries, with environment dependence that interpolates smoothly between these special cases and captures general trends. We shall refer to this theoretically motivated functional form as the Environment Dependent Interatomic Potential (EDIP) for Bulk Si.

#### IV. FUNCTIONAL FORM

Although reasonable interaction potentials can be derived using the analytic methods of the previous section, such inversion schemes become most powerful when used as theoretical guidance for fitting. The reason is that inversion necessarily involves a restricted set of *ab initio* data. Although the input data can be perfectly reproduced (unless it is overdetermined), it is desirable to allow an imperfect description of the inversion data in order to achieve a better overall fit of a wider *ab initio* database that includes low symmetry defect structures. Thus, our approach is to incorporate the theoretically derived features of the previous section directly into our functional form, and then to fit the potential to a carefully chosen *ab initio* database with a minimal number of parameters. In this way, we can systematically derive

a reliable potential for bulk properties while keeping the functional form simple enough to allow for efficient computation of forces as well as intuitive understanding of chemical bonding in covalent solids.

#### A. Scalar Environment Description

The simplest description of the local environment of an atom is the number of nearest neighbors, determined by an effective coordination number  $Z_i$  for atom  $i$ ,

$$Z_i = \sum_{m \neq i} f(R_{im}) \quad (14)$$

where  $f(R_{im})$  is a cutoff function that measures the contribution of neighbor  $m$  to the coordination of  $i$  in terms of the bond length  $R_{im}$ . The special  $sp^2$  and  $sp^3$  bonding geometries can be uniquely specified by their coordinations due to their high symmetry. Since environment dependence is not needed in those cases, it is natural to take the coordination number to be a constant, except when large distortions from equilibrium occur. Moreover, covalent bonds tend to involve only first neighbors, as indicated by *ab initio* charge density calculations of open structures like the diamond lattice<sup>65</sup>. Thus, we choose the neighbor function to be exactly unity for typical covalent bond lengths,  $r < c$ , with a gentle drop to zero above a cutoff  $b$  that excludes second neighbors,

$$f(r) = \begin{cases} 1 & \text{if } r < c \\ \exp\left(\frac{\alpha}{1-x^3}\right) & \text{if } c < r < b \\ 0 & \text{if } r > b \end{cases} \quad (15)$$

where  $x = (r - c)/(b - c)$ . This particular choice of cutoff function is appealing because it has two continuous derivatives at the inner cutoff  $c$ , and is perfectly smooth at the outer cutoff  $b$ . The cutoffs  $b$  and  $c$  are restricted to lie between first and second neighbors of both the hexagonal plane and diamond lattice in equilibrium, so that their coordinations are 3 and 4, respectively.

Our scalar description of the atomic environment is similar to Tersoff’s, but there are notable differences. First, the perspective is that of the atom rather than the bond: With our potential, the preferences for special bond angles, bond strengths and angular forces are the same for all bonds involving a particular atom. This is in contrast to the Tersoff format<sup>9-11,18,29</sup> in which a mixed bond-atom perspective is adopted: the contribution of atom  $i$  to the strength of bond  $(ij)$  is affected by the “interference” of other bonds  $(ik)$  involving atom  $i$ . This model provides an intuitive explanation for trends in chemical reaction paths of molecules<sup>64</sup> and allows for both covalent and metallic bonds to be centered at the same atom, as observed, for example, in *ab initio* charge densities for the BCT5 lattice<sup>65</sup>, which lies between the covalent diamond lattice and the metallic  $\beta$ -tin lattice.

However, the analysis of elastic properties discussed earlier favors the present approach for environment dependence near the diamond lattice. Another important difference between our model and Tersoff's is the separation of angular dependence from the bond order. As we shall see, this allows us to control independently the preferences for bond strengths, bond angles, and angular forces in a way that the Tersoff potential cannot. By keeping the bond order simple, we can also directly use the important theoretical results that motivated the Tersoff potential in the first place.

## B. Coordination-Dependent Chemical Bonding

Our potential consists of coordination-dependent two- and three-body interactions corresponding to the defining features of covalent materials: *pair bonding and angular forces*. The energy of a configuration  $\{\vec{R}_i\}$  is a sum over single-atom energies,  $E = \sum_i E_i$ , each expressed as a sum of pair and three-body interactions

$$E_i = \sum_j V_2(R_{ij}, Z_i) + \sum_{jk} V_3(\vec{R}_{ij}, \vec{R}_{ik}, Z_i), \quad (16)$$

depending on the coordination  $Z_i$  of the central atom. The pair functional  $V_2(R_{ij}, Z_i)$  represents the strength of bond  $(ij)$ , while the three-body functional  $V_3(\vec{R}_{ij}, \vec{R}_{ik}, Z_i)$  represents preferences for special bond angles, due to hybridization, as well as the angular forces that resist bending away from those angles. From our atomic perspective, the pair interaction is broken into a sum of contributions from each atom, and similarly the three-body interaction is broken into a sum over the three angles in each triangle of atoms. Note that due to the environment dependence, the contributions to the bond strength from each pair of atoms are not symmetric in general,  $V_2(R_{ij}, Z_i) \neq V_2(R_{ji}, Z_j)$ .

*Pair Bonding:* We adopt the well-established bond order format of Eq. (6) for the pair interaction. Drawing on the popularity of the SW potential, we use those functional forms for the attractive and repulsive interactions,

$$V_2(r, Z) = A \left[ \left( \frac{B}{r} \right)^\rho - p(Z) \right] \exp \left( \frac{\sigma}{r-a} \right), \quad (17)$$

which go to zero at the cutoff  $r = a$  with all derivatives continuous. This choice can reproduce the shapes of inverted pair potentials for silicon<sup>41</sup>. Because we have constructed  $Z$ , and hence  $p(Z)$ , to be constant near the diamond lattice, our pair interaction reduces exactly to the SW form for configurations near equilibrium, thus allowing us to obtain excellent elastic properties as explained above. Making this choice of repulsive term with the parameters obtained by fitting to defect structures<sup>6</sup>, we can follow the procedure of Bazant and Kaxiras<sup>41</sup> to extract the implied bond order  $p(Z)$  from *ab initio* cohesive energy curves for the following crystal structures

(with coordinations given in parentheses): graphitic (3), diamond (4), BC-8 (4), BCT-5 (5),  $\beta$ -tin (6), SC (6) and BCC (8). These structures span the full range from three and four-fold coordinated covalent bonding in  $sp^2$  and  $sp^3$  arrangements, to overcoordinated atoms in metallic phases. The inverted *ab initio* bond order versus coordination is shown in Fig. 1, along with two additional data points. Since we have only first neighbor interactions in the diamond lattice, we can obtain another bond order for three-fold coordination from the *ab initio* formation energy (3.3 eV) for an unrelaxed vacancy. An additional data point for unit coordination comes from the experimental binding energy (3.24 eV) and bond length (2.246 Å) of the Si<sub>2</sub> molecule<sup>66</sup>.

The bond order data has a clear shoulder at  $Z = Z_0 = 4$  where the predicted transition from covalent to metallic bonding occurs. For overcoordinated atoms with  $Z > Z_0$ , the bond order approaches its rough asymptotic behavior,  $p \propto Z^{-1/2}$ , characteristic of metallic band structure. For coordinations  $Z \leq Z_0$ , the bond order departs from the  $Z^{-1/2}$  divergence, due to the formation of a band gap in the LDOS associated with covalent bonds. A natural choice to capture this shape is a Gaussian,  $p(Z) = e^{-\beta Z^2}$ . In Fig. 1, we see that the bond order function we obtain from fitting<sup>6</sup> is fairly close to the inversion data. It is intentionally somewhat too large for coordinations 5–8 to compensate for the small, but nonvanishing many-body energy for those structures, as described below. The collapse of the attractive functions  $\phi_A(r) = (V_2(r, Z) - V_A(r))/p(Z)$  with this choice of bond order shown in Fig. 2 is reasonably good, thus justifying the bond order formalism across a wide range of volumes. Our potential is the first to have a bond order in such close agreement with theory, which is a direct result of our novel treatment of angular forces.

*Angular Terms:* In a thorough comparative study of Si potentials, Balamane *et al.* attribute the limitations of empirical models to the inadequate description of angular forces<sup>3</sup>. Our potential contains a number of innovations in handling angular forces, leading to a significant improvement over existing models in reproducing *ab initio* data. Analysis of elastic properties shows that, at least near equilibrium, the three-body functional should be expressed as a single, separable product of a radial function  $g(r)$  for both bonds and an angular function  $h(\theta, Z)$ ,

$$V_3(\vec{R}_{ij}, \vec{R}_{ik}, Z_i) = g(R_{ij})g(R_{ik})h(l_{ijk}, Z_i). \quad (18)$$

Although the radial functions could vary with coordination, in the interest of simplicity we have focused on the angular function as the most important source of coordination dependence. Inversion of *ab initio* cohesive energy curves<sup>41</sup> suggests that a consistent choice for the radial functions is the monotonic SW form,

$$g(r) = \exp \left( \frac{\gamma}{r-b} \right), \quad (19)$$



which also goes to zero smoothly at a cutoff distance  $b$ , a value different from the two body cutoff  $a$ . Having separate cutoffs for two and three-body interactions is reasonable because they describe fundamentally different features of bonding. Although the pair interaction might extend considerably beyond the equilibrium first neighbor distance, the angular forces should not be allowed to extend beyond first neighbors, if they are to be interpreted as representing the resistance to bending of covalent bonds.

Much of the new physics contained in our potential comes from the angular function  $h(l, Z)$ . Theoretical considerations lead us to postulate the following general form:

$$h(l, Z) = H\left(\frac{l + \tau(Z)}{w(Z)}\right), \quad (20)$$

where  $H(x)$ ,  $w(Z)$  and  $\tau(Z)$  are generic functions whose essential properties we now describe. The overall shape of the angular function is given by  $H(x)$ , a nonnegative<sup>38,7</sup> function with a quadratic minimum of zero at the origin,  $H(0) = H'(0) = 0$  and  $H''(0) > 0$ . The function  $H(x)$  should also become flat away from the minimum well at the origin, resulting in zero angular force for large distortions away from equilibrium. This feature, which is absent in most potentials including SW, is essential for the angular term to have physical meaning far from equilibrium. When covalent bonds are strongly bent from their equilibrium angle they are weakened and replaced by new electronic states. Thus, for large angular distortions it is not possible to define a restoring force that drives atoms back towards an equilibrium bond angle. These properties of  $H(x)$  can be satisfied by the following choice,

$$H(x) = \lambda\left(1 - e^{-x^2}\right), \quad (21)$$

which is similar in shape to the MFF angular function<sup>28</sup>. However, our angular dependence is considerably more sophisticated than MFF due to its environment dependence.

Motivated by theory, we choose the function  $\tau(Z)$  to control the coordination-dependent minimum of the angular function,  $l_0(Z) = \cos(\theta_0(Z)) = -\tau(Z)$ , with the following form<sup>61,62</sup>,

$$\tau(Z) = u_1 + u_2(u_3 e^{-u_4 Z} - e^{-2u_4 Z}). \quad (22)$$

The parameters,  $u_1 = -0.165799$ ,  $u_2 = 32.557$ ,  $u_3 = 0.286198$ , and  $u_4 = 0.66$ , were chosen to make the preferred angle  $\theta_0(Z) = \cos^{-1}[-\tau(Z)]$  interpolate smoothly between several theoretically motivated values, as shown in Fig. 3: We have already argued that  $\tau(4) = 1/3$  and  $\tau(3) = 1/2$  (so that  $sp^3$  and  $sp^2$  bonding correspond to the diamond and graphitic structures respectively), which determines two of the four parameters in  $\tau(z)$ . The remaining two parameters were selected so that  $\tau(2) = \tau(6) = 0$  or  $\theta_0(2) = \theta_0(6) = \pi/2$ . For

two-fold coordination, this choice reproduces the preference for bonding along two orthogonal  $p$ -states with the low energy, nonbonding  $s$  state fully occupied. For six-fold coordination, the choice  $\theta_0(6) = \pi/2$  also reflects the  $p$  character of the bonds. However, structures with  $Z = 6$  like SC and  $\beta$ -tin are metallic, with delocalized electrons that tend to invalidate the concept of bond-bending underlying the angular function, a crucial point we shall address shortly. The vanishing many-body energies for the graphitic plane and diamond structures allow fitting of the pair interactions  $V_2(r, 3)$  and  $V_2(r, 4)$  to be guided by Eq. (10), which determines  $V_2''(r_d, 4)$  from the bulk modulus, and Eq. (12), which requires  $V_2''(r_h, 3)/V_2''(r_d, 4) \approx 1.4$ . Moreover, the shifting of the minimum of the angular function in our model incorporates coordination-dependent hybridization in a way that other potentials cannot.

Through the function  $w(Z)$ , our angular function has another novel coordination dependence to represent the covalent to metallic transition. The width of the minimum  $w(Z)$  is broadened with increasing coordination, thus reducing the angular stiffness of the bonds as they become more metallic. Similarly, as coordination is decreased from 4 to 3, the width of the minimum is increased to reproduce the smaller angular stiffness of  $sp^2$  bonds compared to that of  $sp^3$  bonds. Thus, the function  $w(Z)$  should have a minimum at  $Z_0 = 4$  and diverge with increasing  $Z$ . Fitting of the model can be guided by Eq. (11), which determines  $w(4)$  from the second shear modulus, and by Eq.(13), which requires  $w(3)/w(4) \approx \sqrt{2}$ . The softening of the angular function is important because it allows the decrease in cohesive energy per atom concomitant with overcoordination to be modeled by a weakening of pair interactions. In contrast, cluster potentials like SW penalize overcoordinated structures with increased three-body energy that overcomes the decrease in pair bonding energy. This is an unphysical feature, since overcoordinated structures do not even have covalent bonds, and the many-body energy cannot be viewed as a consequence of stretching  $sp^3$  bonds far from the tetrahedral geometry. In this sense, the reasonably good description of liquid Si (a metal with about 6 neighbors per atom) with the SW potential appears to be fortuitous.

The coordination dependence of our angular function makes it possible for the first time to reproduce the well-known behavior of the bond order. The reason is that the contribution of the three-body functional to the total energy is suppressed for ideal crystals and overcoordinated structures. The shifting of the minimum makes the three-body energy vanish identically for  $sp^2$  and  $sp^3$  hybrids, and the variable width greatly reduces the three-body energy in metallic structures. With the three-body energy suppressed, we can use our knowledge of the bond order for the graphitic, diamond,  $\beta$ -tin and other lattices from inversion of cohesive energy curves to capture the energetics of these structures in the pair interaction, as

described above. Several other potentials have tried to incorporate the bond order predicted from theory, but the uncontrolled many-body energy makes it impossible to connect directly with theory. Our treatment of angular forces is intuitively appealing because the forces primarily model the bending of covalent bonds, with the control of global energetics left to the pair interactions.

Although our model contains a complicated environment dependence, forces can still be evaluated with computational speed comparable to much simpler existing potentials. The coordination dependence introduces an extra loop into each force calculation. For the three-body functional, this introduces a fourth nested loop over atoms  $m$  outside each triplet  $(ijk)$  that contribute to coordination of atoms  $i$ , which would make force evaluation much slower than the typical three-body cluster expansions used in most other potentials. However, our choice of  $f(r)$  greatly reduces the frequency of four body computations because nonzero forces result if the fourth atom lies in the range of being a partial neighbor,  $c < r_{im} < b$ , which happens only for a small number of neighbors in most cases. If coordinations stay relatively constant during a simulation, as in a low temperature solid, the four-body force computation is insignificant. Indeed, we have found that force evaluation with our model can be almost as fast as with the SW potential<sup>6</sup>, which is an advantage of our model over others of comparable sophistication.

## V. CONCLUSION

In summary, we have used recent theoretical innovations to arrive at a functional form that describes the dependence of chemical bonding on the local coordination number. Bond order, hybridization, metalization and angular stiffness are all described in qualitative agreement with theory. Consistent with our motivation, we have kept the form as simple as possible, reproducing the essential physics with little more complexity than existing potentials. The fitted implementation of the model described in the companion paper<sup>6</sup> involves only 13 adjustable parameters. Using the results of the present article, we provide theoretical estimates of almost half of the parameters, thus greatly narrowing the region of parameter space to be explored during fitting. The remaining parameters are chosen to fit important bulk defect structures.

Considering the theory behind our model, we can anticipate its range of applicability. We have shown that the structure and energetics of the diamond lattice can be almost perfectly reproduced. Because small distortions of  $sp^3$  hybrids are accurately modeled, we would also expect a good description of the amorphous phase. Defect structures involving  $sp^2$  hybridization should also be well described. In general, the model should perform best whenever the coordination number can adequately specify the local atomic environment. This certainly includes

$sp^2$  and  $sp^3$  hybridization and some metallic states, but might also include more general situations in which atoms are more or less symmetrically distributed, like the liquid and amorphous phases and reconstructed dislocation cores and grain boundaries. The theory behind the model begins to break down for noninteger coordinations, since our effective coordination number is a way of smoothly interpolating between well-understood local structures. More seriously, no attempt is made to handle asymmetric distributions of neighbors, which are abundant in surfaces and small clusters. Theory suggests that our model may be fitted to provide a good description of condensed phases and defects in bulk tetrahedral semiconductors, such as Si, Ge and with minor extensions perhaps alloys such as SiGe, that can be understood in terms of simple principles of covalent bonding.

## ACKNOWLEDGMENTS

Partial support was provided to MZB by a Computational Science Graduate Fellowship from the Office of Scientific Computing of the U.S. Department of Energy and to JFJ by the Brazilian Agency CNPq and by the MRSEC Program of the National Science Foundation under award number DMR 94-00334.

- 
- <sup>1</sup> P. Hohenberg and W. Kohn, Phys. Rev. **136**, 864 (1964); W. Kohn and L. J. Sham, Phys. Rev. **140**, 1133 (1965).
  - <sup>2</sup> M. C. Payne, M. P. Teter, D. C. Allan, T. A. Arias, and J. D. Joannopoulos, Rev. Mod. Phys. **64**, 1045 (1992).
  - <sup>3</sup> H. Balamane, T. Halicioglu, and W. A. Tiller, Phys. Rev. B **46**, 2250 (1992); T. Halicioglu, H. O. Pamuk and S. Erkoc, Phys. Stat. Sol. B **149**, 81 (1988).
  - <sup>4</sup> S. J. Cook and P. Clancy, Phys. Rev. B **47**, 7686 (1993).
  - <sup>5</sup> E. Kaxiras, Comp. Mater. Sci. **6**, 158 (1996).
  - <sup>6</sup> J. F. Justo, M. Z. Bazant, E. Kaxiras, V. V. Bulatov, and S. Yip, in preparation.
  - <sup>7</sup> A. E. Carlsson, Solid State Physics **43**, 1 (1990).
  - <sup>8</sup> F. H. Stillinger and T. A. Weber, Phys. Rev. B **31**, 5262 (1985).
  - <sup>9</sup> J. Tersoff, Phys. Rev. Lett. **56**, 632 (1986).
  - <sup>10</sup> J. Tersoff, Phys. Rev. B **37**, 6991 (1988).
  - <sup>11</sup> J. Tersoff, Phys. Rev. B **38**, 9902 (1988).
  - <sup>12</sup> J. Ferrante, J. R. Smith, and J. H. Rose, Phys. Rev. Lett. **50**, 1385 (1983); J. H. Rose, J. R. Smith and J. Ferrante, Phys. Rev. B **28**, 1835 (1983).
  - <sup>13</sup> G. C. Abell, Phys. Rev. B **31**, 6184 (1985).
  - <sup>14</sup> D. G. Pettifor, Springer Proc. in Physics **48**, 64 (1990).
  - <sup>15</sup> R. Biswas and D. R. Hamann, Phys. Rev. Lett. **55**, 2001 (1985); Phys. Rev. B **36**, 6434 (1987).
  - <sup>16</sup> E. Kaxiras and K. Pandey, Phys. Rev. B **38**, 12736 (1988).
  - <sup>17</sup> J. R. Chelikowsky, Phys. Rev. Lett. **60**, 2669 (1988).
  - <sup>18</sup> B. W. Dodson, Phys. Rev. B **35**, 2795 (1987).

- <sup>19</sup> K. E. Khor and S. Das Sarma, Phys. Rev. B **38**, 3318 (1988); **39**, 1188 (1989); **40**, 1319 (1989).
- <sup>20</sup> D. W. Brenner, Phys. Rev. Lett. **63**, 1022 (1989). Brenner shows how the Tersoff format is equivalent to the Embedded Atom Method of Ref.<sup>21</sup>.
- <sup>21</sup> M. I. Baskes, Phys. Rev. Lett. **59**, 2666 (1987); M. I. Baskes, J. S. Nelson and A. F. Wright, Phys. Rev. B **40**, 6085 (1989).
- <sup>22</sup> J. Wang and A. Rockett, Phys. Rev. B **43**, 12571 (1991).
- <sup>23</sup> P. N. Keating, Phys. Rev. **145**, 637 (1966).
- <sup>24</sup> D. W. Brenner and B. J. Garrison, Phys. Rev. B **34**, 1304 (1986).
- <sup>25</sup> A. M. Stoneham, V. T. B. Torres, P. M. Masri and H. R. Schober, Phil. Mag. A **58**, 93 (1988).
- <sup>26</sup> J. N. Murrell and J. A. Rodrigues-Ruiz, Mol. Phys. **71**, 823 (1990); A. R. Al-derzi, R. L. Johnston, J. N. Murrell and J. A. Rodrigues-Ruiz, Mol. Phys. **73**, 265 (1991).
- <sup>27</sup> E. M. Pearson, T. Takai, T. Halicioglu and W. A. Tiller, J. Crystal Growth **70**, 33 (1984).
- <sup>28</sup> A. D. Mistriotis, N. Flytzanis, and S. C. Farantos, Phys. Rev. B **39**, 1212 (1989).
- <sup>29</sup> B. Bolding and H. Anderson, Phys. Rev. B **41**, 10568 (1990).
- <sup>30</sup> D. F. Richards and J. B. Adams, in *Grand Challenges in Computer Simulation*, Proceedings High Performance Computing '95, ed. by A. Tentner, 218 (1995).
- <sup>31</sup> D. F. Richards, J. B. Adams, J. Zhu, L. Yang, and C. Mailhot, Bull. Am. Phys. Soc. **41**, 264 (1996).
- <sup>32</sup> J. R. Chelikowsky J. C. Phillips, M. Kamal and M. Strauss, Phys. Rev. Lett. **62**, 292 (1989); J. R. Chelikowsky and J. C. Phillips, Phys. Rev. B **41** 5735 (1990); J. R. Chelikowsky, K. M. Glassford and J. C. Phillips, **44** 1538 (1991).
- <sup>33</sup> J. S. McCarly and S. T. Pantelides, Bull. Am. Phys. Soc. **41**, 264 (1996).
- <sup>34</sup> J. Harris, Phys. Rev. B **31**, 1770 (1985); A. P. Sutton, M. W. Finnis, D. G. Pettifor and Y. Ohta, J. Phys. C **21**, 35 (1988).
- <sup>35</sup> P. Alinaghian, S. R. Nishitani and D. G. Pettifor, Phil. Mag. B **69**, 889 (1994); A. P. Horsfield, A. M. Bratkovsky, M. Fearn, D. G. Pettifor and M. Aoki, Phys. Rev. B **53**, 12694 (1996).
- <sup>36</sup> A. E. Carlsson, P. A. Fedders and C. W. Myles, Phys. Rev. B **41**, 1247 (1990).
- <sup>37</sup> A. E. Carlsson, Springer Proc. in Phys. **48**, 257 (1990).
- <sup>38</sup> A. E. Carlsson, Phys. Rev. B **32**, 4866 (1985); A. E. Carlsson and N. W. Ashcroft, **27**, 2101 (1983).
- <sup>39</sup> W. A. Harrison, Phys. Rev. B, **41**, 6008 (1990).
- <sup>40</sup> The expansion parameters in these studies are the dimensionless ratios of high to low order moments of the TB LDOS, which may not be small, especially for defect structures with states in the band gap or for metallic states like the liquid, the  $\beta$ -tin crystal structure, and certain surfaces. Low order moments do capture general trends in energy, but cannot be expected to maintain quantitative accuracy.
- <sup>41</sup> M. Z. Bazant and E. Kaxiras, Phys. Rev. Lett., **77**, 4370 (1996).
- <sup>42</sup> M. Z. Bazant and E. Kaxiras, in *Materials Theory, Simulations and Parallel Algorithms*, ed. by E. Kaxiras, J. Joannopoulos, P. Vashista, and R. Kalia, Materials Research Society Symposia Proceedings, **408** (M. R. S., Pittsburgh, 1996), 79.
- <sup>43</sup> A. E. Carlsson, C. Gelatt, and H. Ehrenreich, Phil. Mag. A **41** (1980).
- <sup>44</sup> M. Z. Bazant and E. Kaxiras, in preparation.
- <sup>45</sup> E. R. Cowley, Phys. Rev. Lett. **60**, 2379 (1988).
- <sup>46</sup> A. E. H. Love, *Mathematical Theory of Elasticity*, 4th ed. (Cambridge University Press, 1927).
- <sup>47</sup> M. Born and K. Huang, *Dynamical Theory of Crystal Lattices* (Clarendon Press, Oxford, 1954).
- <sup>48</sup> H. B. Huntington, Solid State Physics **7**, 213 (1958).
- <sup>49</sup> A. H. Cottrell, *The Mechanical Properties of Matter* (Kreiger, New York, 1981).
- <sup>50</sup> M. Born, Ann. Physik **44**, 605 (1914).
- <sup>51</sup> M. Born, in *Lattice Dynamics*, ed. by R. F. Wallis (Pergamon, New York, 1965), 5.
- <sup>52</sup> J. de Launay, Solid State Physics **2**, 220 (1956).
- <sup>53</sup> W. A. Harrison, Ph.D. Dissertation, University of Illinois, Urbana, Illinois (1956).
- <sup>54</sup> G. Simmons and H. Wang, *Single Crystal Elastic Constants and Calculated Aggregate Properties: A Handbook* (MIT, Cambridge, MA, 1971).
- <sup>55</sup> N. Bernstein and E. Kaxiras, submitted to Phys. Rev. B; in *Materials Theory, Simulations and Parallel Algorithms*, ed. by E. Kaxiras, J. Joannopoulos, P. Vashista, and R. Kalia, Materials Research Society Symposia Proceedings, **408** (M. R. S., Pittsburgh, 1996), 55.
- <sup>56</sup> Note that the angular function of the third Tersoff potential<sup>11</sup>, which was specifically optimized for elastic properties, resembles the SW angular function while the other versions do not.
- <sup>57</sup> W. A. Harrison, *Electronic Structure and the Properties of Solids* (Dover, N.Y. 1980).
- <sup>58</sup> Although the covalent bonds in a graphitic plane resemble those around three-fold coordinated atoms in the bulk, we note that the out-of-plane elastic properties of the graphitic structure (e.g.  $C_{44}$ ) are affected by nearly free  $\pi$  electrons which do not participate in the covalent  $sp^2$  hybrid states<sup>57</sup>. These extra electrons, one per atom, try to stay in perpendicular  $p$ -like orbitals, thus contributing to the rigidity of the plane. Nevertheless, we expect the dominant mechanical behavior of three-fold coordinated bulk defect atoms to be quite similar to atoms in a graphitic plane.
- <sup>59</sup> J. F. Nye, *Physical Properties of Crystals* (Clarendon Press, Oxford, 1957).
- <sup>60</sup> We calculated the DFT/LDA elastic moduli for an isolated hexagonal plane using a plane wave basis with a 12 Ry cutoff and 1296 points in the full Brillouin zone for reciprocal space integrations. These choices guarantee sufficient accuracy. In order to preserve periodic boundary conditions, the out-of-plane lattice parameter was fixed at  $c = 5.5 \text{ \AA}$ , which is large enough to ensure negligible interplanar forces. The parabolic regime of the energy versus strain data (typically, strains less than 3%) was isolated by considering the goodness of parabolic fit, as measured by the  $\chi^2$  statistic.
- <sup>61</sup> S. Ismail-Beigi and E. Kaxiras, private communication (1993).
- <sup>62</sup> Khor and Das Sarma used a shifted equilibrium bond angle within the Tersoff format, but they did not specify exactly how the equilibrium angle should depend on the local en-

vironment in a general configuration<sup>19</sup>.

<sup>63</sup> See Fig. 2 of Carlsson<sup>7</sup>.

<sup>64</sup> D. W. Brenner, M.R.S. Bulletin, **21**, 36 (1996).

<sup>65</sup> E. Kaxiras and L. L. Boyer, Modeling Simul. Mater. Sci.

Eng. **1**, 91 (1992).

<sup>66</sup> K. P. Huber and G. Herzberg, *Constants of Diatomic Molecules* (Van Norstrand, New York, 1979).

TABLE I. Comparison of elastic constants (in units of Mbar) for diamond cubic silicon computed from empirical models with experimental or *ab initio* (LDA) values. The values for experiment (EXPT) are from Simmons and Wang<sup>54</sup>, for tight-binding (TB) from Bernstein and Kaxiras<sup>55</sup> and for the empirical potentials Biswas-Haman (BH), Tersoff (T2, T3), Dodson (DOD) and Pearson-Takai-Halicioglu-Tiller (PTHT) from Balamane<sup>3</sup>. The Stillinger-Weber (SW) values were calculated with the analytic formulae of Cowley<sup>45</sup> and scaled to set the binding energy to 4.63 eV<sup>3</sup>. In the lower half of the table, we test the elastic constant relations discussed in the text by calculating the ratios  $\alpha_H \equiv (7C_{11} + 2C_{12})C_{44}/3(C_{11} + 2C_{12})(C_{11} - C_{12})$  and  $\alpha_B \equiv (4C_{11} + 5C_{12})/9C_{44}^0$ .

	EXPT	LDA	SW	BH	T2	T3	DOD	PTHT	TB
$C_{11}$	1.67		1.617	2.042	1.217	1.425	1.206	2.969	1.45
$C_{12}$	0.65		0.816	1.517	0.858	0.754	0.722	2.697	0.845
$C_{44}$	0.81		0.603	0.451	0.103	0.690	0.659	0.446	0.534
$C_{44}^0$		1.11	1.172	1.049	0.923	1.188	3.475	2.190	1.35
$\alpha_H$	1.16		1.00	0.98	2.99	2.31	1.69	1.71	2.80
$\alpha_B$		0.99	1.00	1.67	1.10	0.89	0.27	1.29	0.82

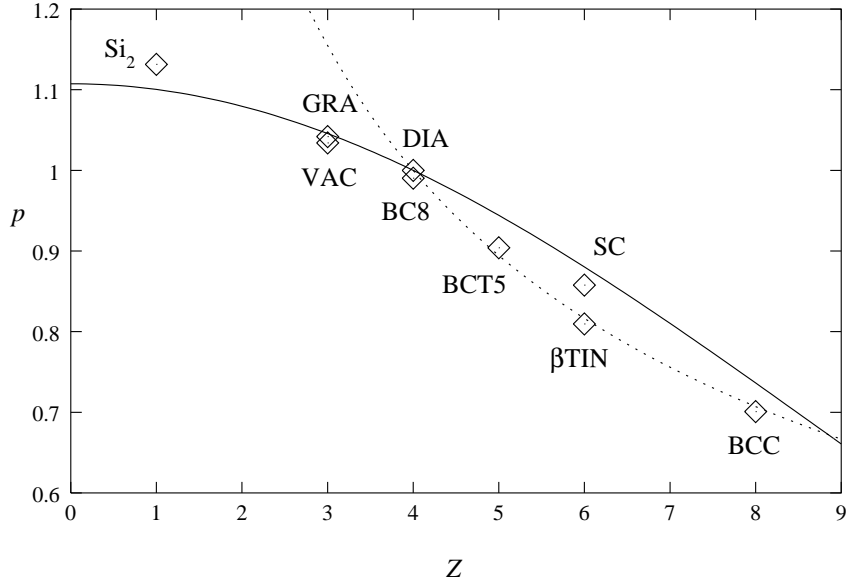


FIG. 1. *Ab initio* values for the bond order as a function of coordination, obtained from the inversion of cohesive energy curves for the graphitic (GRA), cubic diamond (DIA), BC8, BCT5, SC,  $\beta$ -tin and BCC bulk structures and with additional points for the unrelaxed vacancy (VAC) and the dimer molecule ( $\text{Si}_2$ ), as explained in the text. For comparison the solid line shows the Gaussian  $p(Z)$  obtained from fitting to defect structures. The dotted line shows the  $1/\sqrt{Z}$  dependence, the theoretically predicted approximate behavior for large coordinations.

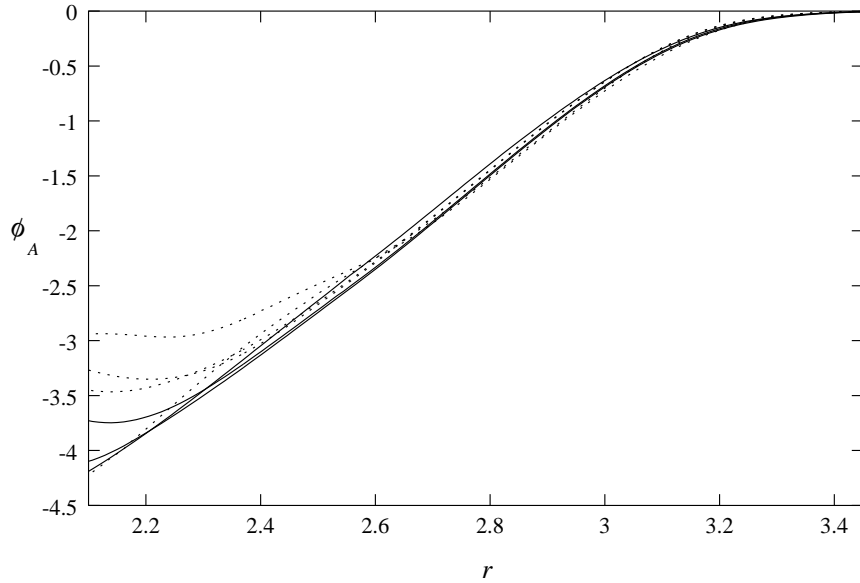


FIG. 2. Attractive pair interactions from inversion of *ab initio* cohesive energy curves for the structures in Fig. 1 using the bond order and repulsive pair potential of our model. The solid lines are for the covalent structures with coordinations 3 and 4, while the dotted lines are for the overcoordinated metallic structures. The reasonable collapse of the attractive pair potentials indicates the validity of the bond order functional form of the pair interaction across a wide range of volumes and crystal structures.

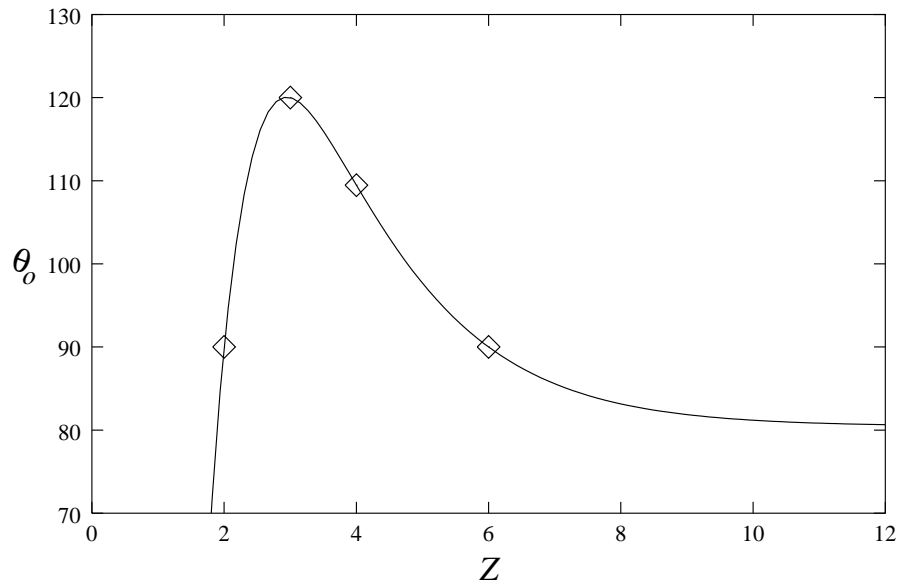


FIG. 3. The coordination dependence of the preferred bond angle  $\theta_o(Z)$  (in degrees), which interpolates the theoretically motivated points for  $Z = 2, 3, 4, 6$ , indicated by diamonds.